



Published in final edited form as:

Nanomedicine. 2009 September ; 5(3): 305–315. doi:10.1016/j.nano.2008.11.003.

Factorial Analyses of Photopolymerizable Thermoresponsive Composite Hydrogels for Protein Delivery

Abhimanyu Sabnis, MS^{1,†}, Aniket S. Wadajkar, MS^{1,†}, Pranesh Aswath, PhD², and Kytai T. Nguyen, PhD^{1,*}

¹Department of Bioengineering, University of Texas Southwestern Medical Center at Dallas and University of Texas at Arlington

²Department of Material Science, University of Texas at Arlington

Abstract

A smart protein delivery system for wound healing applications was developed using composite nanoparticle hydrogels that can release protein in a temperature-responsive manner. This system can also be formed *in situ* in the presence of ultraviolet light and Irgacure 2959 photoinitiator. The system consists of temperature sensitive poly(*N*-isopropylacrylamide-co-acrylamide) (PNIPAM-AAm) nanoparticles embedded in a poly(ethylene glycol) diacrylate (PEGDA) matrix. A factorial analysis was performed to evaluate the effects of PEGDA concentration (10% and 15% w/v) and PEGDA molecular weight (3.4 kDa and 8 kDa), as well as PNIPAM-AAm nanoparticle concentration (2% and 4% w/v) and temperature (23°C and 40°C) on the protein release profiles and swelling ratios of the hydrogels. Results indicate PNIPAM-AAm nanoparticle concentration and temperature were the most important factors affecting the protein release during the burst release phase. Additionally, PEGDA molecular weight was the most important factor affecting the protein release in the plateau region. It was also an important factor that controlled the hydrogel swelling ratio. A dual layered hydrogel was further developed to produce a protein delivery system with a better sustained release. These findings have improved our understanding of the composite hydrogel systems and will help in tailoring future systems with desired release profiles.

Keywords

photopolymerization; hydrogel; thermoresponsiveness; photo cross-linker; factorial analysis; poly(ethylene glycol) diacrylate; poly(*N*-isopropylacrylamide-co-acrylamide); protein delivery; swelling ratio

Introduction

Photo cross-linking hydrogels, incorporated with therapeutic agents, have been investigated extensively as drug delivery systems since the major benefit of these hydrogels is that they can be formed *in-situ* at a specific site by photopolymerization [1]. Various photopolymerizable

*Corresponding author: Address: University of Texas at Arlington, Department of Bioengineering, 501 West First Street, ELB 220, Arlington, TX 76010, Phone: 817-272-2540, Fax: 817-272-2251, Email: knguyen@uta.edu.

[†]Both authors contributed equally

There is no potential, perceived or real conflict of interest.

Publisher's Disclaimer: This is a PDF file of an unedited manuscript that has been accepted for publication. As a service to our customers we are providing this early version of the manuscript. The manuscript will undergo copyediting, typesetting, and review of the resulting proof before it is published in its final citable form. Please note that during the production process errors may be discovered which could affect the content, and all legal disclaimers that apply to the journal pertain.

polymers have been studied. Examples include (di)methacrylic or (di)acrylic derivatives of poly(ethylene glycol) (PEG) [2,3], poly(ethylene oxide) [4,5], poly(vinyl alcohol) [6], and diethyl fumarate/poly(propylene fumarate) [7]. Of the photo cross-linking hydrogels, poly(ethylene glycol) (PEG)-based materials are widely investigated for biomedical applications due to their advantageous properties such as biocompatibility, low immunogenicity, and the ease of use [8-14]. PEG functionalized with diacrylate (PEGDA) or dimethacrylate groups cross-link to form nondegradable hydrogels that are used in various biomedical applications such as the microencapsulation of islets [9,10], controlled release vehicles [3,15], adhesion prevention barriers [8,16], and bone restorations [11].

In addition to photo cross-linking hydrogels, environmentally responsive drug delivery systems have also been investigated for controlled drug delivery applications. Such stimuli-responsive systems undergo phase transitions in response to changes in ionic strength, pH, light, electric field, irradiation, or temperature [17]. In particular, among the temperature-sensitive hydrogels reported to date, poly(*N*-isopropylacrylamide) (PNIPAM) and its copolymers have been widely used for pharmaceutical and tissue engineering applications because of their thermal properties [18]. For example, the release of drugs embedded in these hydrogels can be controlled by changing the local temperature [17]. The unique property of PNIPAM to undergo a reversible phase transition at temperatures close to body temperature makes it desirable for biomedical applications [19-23]. This phase transition occurs in aqueous solutions at a lower critical solution temperature (LCST) around 32°C for PNIPAM. At temperatures below the LCST, PNIPAM exhibits hydrophilic properties and exists in an individual chain with a coil conformation. Above the LCST, hydrophobic attractions become more favorable, resulting in a sharp transition from the coil to globule conformation, leading to the collapse of the structure to release drugs from the material [24]. The LCST of PNIPAM can be further increased to above body temperature by copolymerizing with hydrophilic monomers such as PEG [24,25] and acrylamide (AAm) [26].

In this study we combined both photopolymerizable and thermoresponsive hydrogels to develop a composite hydrogel system for drug/protein delivery applications. This system can be formed at a specific location *in-situ* via photopolymerization and the drug release from this system can be controlled by changing the temperature locally. The principle of the system, shown in Figure 1, can be briefly described as follows. A precursor solution comprised of the drug- or protein-loaded PNIPAM-acrylamide (PNIPAM-AAm) nanoparticles, photoinitiators (Irgacure 2959), and photo cross-linkers (PEGDA) would be delivered at the injured or wound site. In the presence of ultraviolet (UV) light these materials would form a hydrogel network entrapping the PNIPAM-AAm nanoparticles at the injured site to form a protective barrier. When the local temperature is increased to or above the LCST (39-40°C), the PNIPAM-AAm nanoparticles would undergo a reversible phase transition, collapse, and expel the drugs or proteins into the surrounding tissue.

Controlled release studies of proteins and/or drugs from temperature sensitive PNIPAM bulk gels and PNIPAM nanoparticle networks have been previously investigated. For example, PNIPAM gels have been used for controlled release of drugs and proteins in response to changes in temperature [27-30]. In addition, PNIPAM nanoparticle networks by either covalently crosslinking neighboring particles or a seed-and-feed method [31,32] have also been developed for loading and releasing drugs/proteins. In contrast to these drug delivery systems, our current strategy of controlled release is to first load PNIPAM-AAm nanoparticles with drugs/proteins and then to entrap drug-loaded nanoparticles within the PEGDA hydrogel. Delivery of bioactive molecules such as proteins, genes, and peptides would be a potential benefit of this composite hydrogel system compared to other drug delivery carriers as these molecules are easily denatured by extreme heat and organic solvents [33]. These molecules are also released quickly if they are directly loaded in the bulk hydrogels. In contrast, the PEG

hydrogel cross-linking density and thermoresponsive property of PNIPAM-AAm nanoparticles in our system might affect the release of such bioactive molecules, thus providing a more controlled and sustained release of these molecules.

The aim of this study was to investigate the system characteristics, such as protein release and hydrogel swelling ratio, in response to changes in different factors (PEGDA molecular weight, PEGDA concentration, PNIPAM-AAm nanoparticle concentration, and temperature) using a factorial design approach. In addition, a double layer hydrogel with the inner layer containing the protein was developed to examine the role of a diffusion layer on the protein release characteristics.

Methods

Materials

Chemicals, if not specified, were purchased from Sigma-Aldrich (St. Louis, MO), including poly(ethylene glycol), anhydrous dichloromethane, triethylamine, acryloyl chloride, potassium carbonate, magnesium sulfate, ethyl ether, *N*-isopropylacrylamide, *N*, *N*'-methylenebisacrylamide, potassium persulfate, and sodium dodecyl sulfate.

Preparation of Poly(ethylene glycol) diacrylate (PEGDA)

The factorial design of the hydrogel system required evaluation of two molecular weights (MW) (3.4 kDa and 8 kDa) of the cross-linker polymer, PEGDA. PEGDA was synthesized by modifying the previously described methods [34,35]. In brief, 12 g of poly(ethylene glycol) (3.4 kDa or 8 kDa) was dissolved in 36 ml of anhydrous dichloromethane. 1.3 ml of triethylamine was added to the flask and the solution was bubbled with argon gas for 5 minutes. 0.61 ml of acryloyl chloride was then dissolved in 10 ml of dichloromethane and added drop by drop slowly (over an hour or two) to the flask. The solution was stirred under argon for 2 days on an ice bath. The solution was then washed with 2M K₂CO₃ to separate the dichloromethane phase, followed by drying with anhydrous MgSO₄. PEGDA was then precipitated using ethyl ether. Finally, the product was filtered and dried for 12 hours under vacuum at room temperature.

Preparation of Poly(*N*-isopropylacrylamide-co-acrylamide) (PNIPAM-AAm) Nanoparticles

PNIPAM-AAm nanoparticles (100 nm in size) with the volume transition temperature of 39.2° C were prepared by modifying the previously described methods [1,26,36]. An aqueous solution (100 ml) containing *N*-isopropylacrylamide (1.3644 g), acrylamide (0.1756 g), *N*, *N*'-methylenebisacrylamide (0.0262 g), and sodium dodecyl sulfate (0.0439 g) was stirred under argon gas for 30 minutes. Potassium persulfate (0.0624 g) was added and radical polymerization was carried out at 70°C for 4 hours under argon. The resulting particles were cooled to room temperature and dialyzed (6-8 kDa MW cutoff) against deionized water for 4 days to remove unreacted monomers and surfactants.

Factorial Analysis using Design of Experiments

The factorial studies utilized Design Expert, a design of experiments (DOE) software from Stat-Ease, to elucidate the effect of individual and multiple factors on the protein release rate and swelling ratio of the composite hydrogel system. Using DOE, it was possible to design a half-factorial experiment (8 instead of 16 runs) for four factors for the protein release experiments. The four factors (independent variables) included the PEGDA MW (3.4 kDa and 8 kDa), PEGDA concentration (10% and 15% w/v), PNIPAM-AAm nanoparticle concentration (2% and 4% w/v), and temperature (23°C and 40°C). For the hydrogel swelling experiments, a half-factorial experiment (4 instead of 8 runs) for three factors (temperature

was constant at 23°C) was designed. The evaluated responses (dependent outcomes) included the protein release rate and the swelling ratio of the hydrogels. The resulting factorial design is shown in Tables 1-3. PEGDA molecular weight, PEGDA concentration, PNIPAM-AAm nanoparticle concentration, and temperature are represented as M, P, N, and T, respectively.

Preparation of Photopolymerized Thermoresponsive Hydrogels

PNIPAM-AAm nanoparticles were dispersed in deionized water to get a stock suspension. Bovine serum albumin (BSA), as a model protein, was added to the stock suspension at a concentration of 5% (w/v) and incubated at 4°C for 4 days. Hydrogels (n=4 for each run) for the factorial analysis were prepared based on Table 2. For example, run 1 was prepared by dissolving 0.1 g of PEGDA (3.4 kDa) in 800 µl of BSA-loaded PNIPAM-AAm nanoparticle suspension. 200 µl of the photoinitiator stock solution (0.0125 g/ml) was then added to this solution to make 1 ml total solution with final PEGDA and PNIPAM-AAm nanoparticle concentrations of 10% (w/v) and 2% (w/v), respectively. To form the hydrogel, 200 µl of the precursor solution was added to a 48-well plate and exposed to UV light at about 10 mW/cm² for less than 5 minutes. In our previous work, we optimized the concentration of the photoinitiator and duration of UV exposure by evaluating cytotoxic effects of the photoinitiator and UV exposure on fibroblast and smooth muscle cell viability [37].

Effects of Factors on Protein Release

To evaluate the effect of the factors on protein release, protein loaded nanoparticle hydrogels (n=4) for each run were incubated at room temperature (23°C) (below LCST) and at 40°C (above LCST) in 24-well plates with 1 ml of PBS solution. At the pre-determined time points (1, 2, 4, 8, 12, 24, and 48 hours), the PBS solution from the wells was replaced with 1 ml of fresh PBS solution. The samples collected at various time points were then analyzed using the BCA protein assay (Pierce, following manufacturer's instructions) to evaluate the amount of protein released from the hydrogel. The data was analyzed and the protein release profiles for each run at both temperatures were plotted.

Effects of Factors on Swelling Ratio

The swelling ratios for the hydrogels from different runs were determined to better understand how the factors such as PEGDA molecular weight and concentration as well as PNIPAM-AAm nanoparticle concentration affected the hydrogel structure. After photopolymerization, the hydrogels (n=4) were allowed to swell with PBS solution at room temperature for 4 days. These swollen hydrogels were then dried with moistened filter paper and weighed to get the W_S , the swollen weight of the hydrogels. The dry weight of the hydrogels, W_D , was measured after the drying of the hydrogels. The swelling ratio (S.R.) of the hydrogels was calculated using Equation 1.

$$S.R. = \frac{W_S - W_D}{W_D} \quad (1)$$

Midpoint Analysis

Midpoint analysis was performed to confirm the linear dependence of the dependent variables on the independent variables. Approximate mid-levels of three factors other than temperature were chosen and hydrogels were prepared (n=4) for midpoint analysis. For instance, the precursor solution was prepared by selecting a PEGDA molecular weight of 6 kDa and a concentration of 12.5% (w/v) and a PNIPAM-AAm nanoparticle concentration of 3% (w/v). The hydrogels were formed by adding 200 µl of the precursor solution to a 48-well plate and

exposed to UV light at 10 mW/cm². To evaluate the effect of the factors on protein release, hydrogels (n=4) were incubated at room temperature (23°C) and above LCST (40°C) in 24-well plates with 1 ml of PBS solution. Protein release studies were performed as described earlier.

Photopolymerized Thermo-responsive Double Layer Hydrogels

The double layer hydrogels were prepared to tailor the protein release rate and minimize the early burst release. In order to form the double layer hydrogels, single layer hydrogels were first prepared, as previously described, by selecting midpoint values of the factors as mentioned in the midpoint analysis. The single layer hydrogels (n=4), immediately after formation, were immersed in the solution containing PEGDA and the photoinitiator in a 24-well plate. The solution containing hydrogel was then exposed to UV light and photopolymerized to form an additional layer of PEGDA around the nanoparticle composite single layer hydrogel. Protein release studies were performed by incubating double layer hydrogels at 23°C and 40°C to compare with the protein released from single layer hydrogels (prepared for midpoint analysis).

Results

In this study, we developed the composite nanoparticle hydrogel network that can be photopolymerizable in situ and can release drugs in response to changes in local temperature for drug/protein delivery applications (Figure 1). A comparison of two identical composite hydrogel systems maintained at two different temperatures, i.e. 23°C and 40°C, as well as a SEM image of the composite system is shown in Figure 2. We have previously investigated the biocompatibility of our composite nanoparticle hydrogel network [37]. In this research, we evaluated the effects of four factors (PEGDA MW and concentration, PNIPAM-AAm nanoparticle concentration, and temperature) on protein release, thermo-responsiveness, and swelling ratio of the hydrogels. The effects of each factor are presented and discussed in details below,

Effects of Factors on Protein Release

From the protein release data, it was observed that all tests exhibited a triphasic protein release, with an initial burst release (within the first hour) and a sustained burst release (from 1 to 8 hours) followed by a plateau release (up to 48 hours). Most of the protein was released within the first 8 hours of the study (Figure 3). In addition, all tests exhibited a thermo-responsive release behavior with hydrogels at 40°C releasing a significantly higher amount of protein as compared to hydrogels at 23°C, over the same duration.

To better understand the factors that govern the protein release characteristics from the hydrogels, the protein release rates (R) were calculated for the different tests at both temperatures (Table 2). Protein release rates were calculated using Equation 2.

$$\text{Protein Release Rate, } R = \frac{D_2 - D_1}{t_2 - t_1} \quad (2)$$

Where

R is the protein release rate between two time points (µg/hr)

D₁ and D₂ are the amounts of protein released at time t₁ and t₂, respectively (µg)

t₁ and t₂ are time points at which protein release was quantified (hours)

Using the protein release rates, a factorial analysis was performed to evaluate the effect of individual factors on protein release profiles. It was important to evaluate the release kinetics over these three periods, namely, 0 to 1 hour (initial burst), 1 to 8 hours (sustained burst), and 8 to 48 hours (plateau). A half normal probability plot provides information on factors that are important and those that are not. In addition, it provides insight into the relative importance of these factors. As shown in Figure 4a, the absolute value of an effect on the X-axis and estimates of errors are represented as squares and triangles, respectively. The largest effects towards the right of the plot are real effects, while the effects close to the zero region are those that occur by chance and are categorized as errors. The effects are categorized as positive and negative effects. The positive effects represent a direct relationship of the design factors with the system outcomes, while the negative effects represent an inverse relationship. In the burst phase of the release (0-1 hour), the half normal probability plot shown in Figure 4a indicates that the most important factors that control the release of the protein are the temperature, PNIPAM-AAm concentration, and to a lesser extent a combination of the two. The PEGDA concentration (negative effect) and PEGDA molecular weight (positive effect) are less important. In order to gain a better understanding of the relationship between PNIPAM-AAm nanoparticle concentration and temperature on protein release rate, the response surface diagram was developed at a PEGDA molecular weight of 5.7 kDa and a PEGDA concentration of 12.50 % w/v, which lies close to the mid point of the range of both molecular weight and concentration as shown in Figure 4b. From Figure 4b it is evident that increasing the temperature has the single largest effect on burst release. The synergistic effect of temperature and PNIPAM-AAm nanoparticle concentration also plays a significant role in enhancing the protein release rate.

PNIPAM-AAm phase transition above LCST (i.e. a temperature above LCST) is the major factor in deciding the protein release rate. Most of the protein will be released when the PNIPAM-AAm nanoparticles' structures collapse and expel the protein. The equation for protein release rate in the first hour in terms of actual factors and combined effects of factors was obtained from factorial analysis. The predicted protein release can be calculated for any combination of individual factors within the range provided in Table 1 by using Equation 3.

$$R \text{ in the first phase } (\mu\text{g/hr}) = 673.27 + (163.78)M - (108.51)P - (161.21)N + (1.21)T - (4.06)MT + (2.21)PT + (12.75)NT \quad (3)$$

Where

M = PEGDA molecular weight

P = PEGDA concentration

T = temperature

N = PNIPAM-AAm nanoparticle concentration

MT is the combined effect of PEGDA MW and temperature

PT is the combined effect of PEGDA concentration and temperature

NT is the combined effect of PNIPAM-AAm nanoparticle concentration and temperature

In the second phase (sustained burst release, 1-8 hours), PNIPAM-AAm nanoparticle concentration and temperature have positive effects, whereas PEGDA concentration has a significant negative impact on the protein release rate as shown in Figure 4c. A two factor interaction between PNIPAM-AAm nanoparticle concentration and temperature also plays an important role. Figure 4d shows the response surface plot for the dependence of the temperature and PNIPAM-AAm nanoparticle concentration on the protein release rate. The equation for

protein release rate from 1-8 hours, in terms of actual factors and combined effects of factors, was obtained from factorial analysis. The predicted protein release can be calculated for any combination of individual factors within the range provided in Table 1 using Equation 4.

$$R \text{ in the second phase } (\mu\text{g/hr}) = 464.34 + (19.03)M - (26.37)P - (62.58)N + (7.55)T - (0.4)MT + (0.37)PT + (3.52)NT \quad (4)$$

The effects of the factors on the protein release rate in the last phase (sustained release, 8-48 hours) were found to be much different than in the previous two phases. Temperature and its combined effect with PNIPAM-AAm nanoparticle concentration were not the important factors in controlling the protein release rate as shown in the half normal probability plot in Figure 4e. The most dominant factor was the PEGDA molecular weight. A response surface diagram with temperature and PNIPAM-AAm nanoparticle concentration is shown in Figure 4f. The protein release rate at 40°C is independent of the PNIPAM-AAm concentration, while at 23°C, there is still a dependence on the PNIPAM-AAm concentration. It can be postulated that at 40°C, most of the protein has already been released in phase I and II and little is left for release in phase III, resulting in no dependence on the PNIPAM-AAm concentration. On the other hand, at 23°C a significant amount of protein is still present at the end of phase II, and hence, the hydrogels with the higher PNIPAM-AAm concentration have a higher release rate. When PEGDA MW and temperature are considered as variables, the response surface diagram is shown in Figure 4g. It is clearly evident that a higher PEGDA MW results in a higher protein release rate, in particular at 23°C. It is possible that the hydrogels with the higher PEGDA MW allow more diffusion, resulting in a higher protein release rate in phase III.

The equation for the protein release rate from 8-48 hours, in terms of actual factors and combined effects of factors, was obtained from factorial analysis. The predicted protein release can be calculated for any combination of individual factors within the range provided in Table 1 using Equation 5.

$$R \text{ in the third phase } (\mu\text{g/hr}) = -17.74 + (2.75)M + (0.27)P + (4.12)N + (0.6)T - (0.06)MT - (0.0072)PT - (0.097)NT \quad (5)$$

Dependence of Thermoresponsiveness on Factors

One of the main reasons to perform factorial analysis on the photopolymerized hydrogel composite systems was to elucidate the relationship between the factors and the hydrogel thermo-responsive behavior, i.e. the higher protein release at 40°C compared to 23°C. From Figure 3, it is clear that all four pairs of runs showed a significant thermo-responsive behavior. To better understand this effect, the release rate difference between 23°C and 40°C for all four pairs of runs was calculated and is shown in Table 2. The largest impact of the thermo-responsive behavior in release rates was in phase I, or the burst regime of protein delivery. On analyzing the factorial influence on the thermo-responsive behavior, changing PNIPAM-AAm nanoparticle concentration to the high level was found to result in an increase in thermo-responsive behavior (Figure 4h and 4i).

Effects of Factors on Swelling Ratio

To evaluate the effects of the factors, excluding temperature, on the swelling ratio, the swollen weights (W_S) and dry weights (W_D) of the hydrogels ($n=4$) were measured. The swelling ratios of the hydrogels were then calculated using Equation 1. The factorial analysis on the hydrogel swelling ratio revealed that increasing the PEGDA MW from 3.4 kDa to 8 kDa was the most

important factor in increasing the swelling ratio (Figure 5a and 5b). On the other hand, PEGDA concentration and PNIPAM-AAm nanoparticle concentration were found to have a mild, negative effect on the swelling ratio.

Midpoint Analysis and Double Layer Hydrogels

Midpoint analysis was conducted through the protein release study to evaluate the curvilinear effect of dependent factors on the independent factors. The scheme of the double layer hydrogel and the cumulative protein release from single layer (SL) and double layer (DL) hydrogels at 23°C and 40°C are shown in Figure 6a and 6b. Protein release profiles of both types of hydrogels exhibited a thermoresponsive release behavior with hydrogels at 40°C releasing a significantly higher amount of protein, compared to hydrogels at 23°C, over the same time duration. It can be seen that the double layer hydrogels release a significantly smaller amount of protein in a sustained manner compared to the single layer hydrogels.

The protein release studies on composite hydrogels at the midpoint level of the two level factorial design (midpoint analysis) generated similar protein release profiles to the hydrogels of the four run pairs (Figure 6b). The protein release profiles exhibited a triphasic protein release and thermoresponsive release behavior. In addition, the effects of individual and combined factors on protein release profiles during each phase of release and swelling ratio were similar to earlier studies (Figure 4b, 4d, 4g, and 6b). These observations confirm the linear dependence of dependent variables on the independent variables.

Discussion

In this study, we developed the composite nanoparticle hydrogel network that can be UV-polymerized *in situ* within a short time (less than five minutes). This composite hydrogel would also be able to release drugs in response to changes in local temperature for drug/protein delivery applications. As shown in Figure 1, our system consist of the drug- or protein-loaded PNIPAM-acrylamide (PNIPAM-AAm) nanoparticles, photoinitiators (Irgacure 2959), and photo cross-linkers (PEGDA). A hydrogel network can be formulated at any shape or form *in situ* under the presence of UV light. Another major advantage of our current drug delivery system is that when the local temperature is increased to or above the LCST (39-40°C), the PNIPAM-AAm nanoparticles within the composite hydrogel would undergo a reversible phase transition, collapse, and expel the drugs into the surrounding tissue, thus this system can be used for on-off drug delivery mechanism [28,31,32]. Our previous work has shown that this composite nanoparticle hydrogel network is biocompatible [37]. In addition, the temperature within the hydrogel was raised a little from a short-term UV exposure, and this small increase does not cause the denature of proteins loaded within hydrogels [3,15]. In this work, we further determined effects of four major factors, PEGDA MW and concentration, PNIPAM-AAm nanoparticle concentration, and temperature, on protein release, thermoresponsiveness, and swelling ratio of the composite hydrogel system.

The factorial analysis was performed to evaluate the effects of four factors (PEGDA MW and concentration, PNIPAM-AAm nanoparticle concentration, and temperature) on protein release of the hydrogels. In the initial burst (phase I) and sustained burst region (phase II), higher PNIPAM-AAm nanoparticle concentration and higher temperature were shown to result in an increase in protein release, while PEGDA MW governed protein release in the plateau region (phase III). It is reported that with a higher PEGDA concentration there is greater opportunity for cross-links to form [38]. This increased number of cross-links in the higher PEGDA MW might affect the network structure by forming a denser, closer knit network, thereby hindering the protein release in phases I and II (0-8 hours) and resulting in a larger release in phase III (8-48 hours). Similar to our study, other studies also observe the dependence of BSA release on PEGDA molecular weight. For example, 50% total BSA release in 20 hours and 100%

release in 5 days were observed when PEGDA MW 10,000 was used, whereas the total BSA release was reduced significantly (86% of BSA in 270 days) when a PEG MW of 575 was used [3]. In addition, BSA released from PEG hydrogels is often in the monomeric form, whereas the protein aggregates are maintained within the hydrogel matrix and could not be released out of the system [15].

PNIPAM-AAm nanoparticle concentration was the major factor controlling the degree of thermoresponsiveness of the hydrogel systems. Changing PNIPAM-AAm nanoparticle concentration to the high level was found to result in an increase in thermoresponsive behavior (Figure 4h and 4i). As PNIPAM-AAm nanoparticles are the only thermoresponsive components of the system, it is obvious that they would have the greatest effect on the temperature responsiveness of our hydrogel system. In addition, PEGDA molecular weight and PEGDA concentration would have some effect on the thermoresponsiveness by affecting the diffusion of the protein already expelled by nanoparticles, but entrapped in the hydrogel network. Similar to our observation, nanoparticle networks by covalently crosslinking neighboring nanoparticles made of PNIPAM-co-allylamine also exhibit a temperature-dependent release of drugs [31]. Compared to the thermoresponsive bulk hydrogels, drug loading by nanoparticle networks such as our system have more advantages. For instance, drugs are usually loaded in a bulk gel either by mixing the drug with monomers, initiators, and crosslinkers, or by allowing a bulk gel to swell to equilibrium in a concentrated drug solution [39]. These loading approaches might potentially cause damage to the drug and exclude large molecules to be absorbed in a bulk gel. Similar to thermoresponsive nanoparticle networks [39], our thermoresponsive nanoparticle composite hydrogels would allow the drug mixed into the nanoparticle dispersion at room temperature, thereby reducing the above limitation.

PEGDA MW was found to be the most important factor for swelling ratio with higher MW PEGDA having higher swelling ratios. Similar to our studies, DiRamio et al. have also shown that the swelling ratios increased as the molecular weight of the cross-linker increased for their PEG methacrylate/dimethacrylate hydrogels [40]. Evaluating the hydrogel swelling ratios was important as it further corroborated the theory that the lower MW cross-linker would have shorter chains than the higher MW cross-linker, and thus form a tighter, more compact network due to the larger number of cross-links. Therefore, a lower MW cross-linker will not allow the hydrogel to swell sufficiently (compared to the higher MW), and hence, diffusion of water into and protein out of the hydrogel would be limited. This explains how increasing the PEGDA MW had a positive effect on the protein release, especially in phase III (Figure 4g) where a significant portion of the protein is already released and the remaining protein release is controlled by the diffusion mechanism.

In general, our results indicate that both PNIPAM-AAm nanoparticle concentration and temperature govern protein release in the burst region, while PEGDA MW controls protein release in the plateau region. In addition, PNIPAM-AAm nanoparticle concentration plays an important role in controlling the degree of thermoresponsiveness, whereas PEGDA MW is the most important factor for swelling ratio of our composite hydrogel system. The outcome of this study is that a composite hydrogel system could be tailored to obtain desired characteristics such as drug release profiles and swelling. Furthermore, a sustained release of therapeutic agents can be achieved by adding another layer of PEGDA on top of the composite hydrogel. DL hydrogels consist of an outer layer of PEGDA that was protein-free surrounding and the inner layer of PEGDA that contained the protein-loaded PNIPAM-AAm nanoparticles. Results of protein release from DL hydrogels indicate that the protein released from PNIPAM-AAm nanoparticles slowly diffused first through the PEGDA network and then through the outer layer of PEGDA. Thus, the double layer hydrogels could be used as a mean to provide a more sustained and controlled drug/protein release in response to changes in temperature compared to single layer hydrogels.

Acknowledgments

We acknowledge financial support from the American Heart Association Scientist Development Award 073520N and NIH grants HL082644 and HL091232 (K.N.).

References

1. Ramanan R, Chellamuthu P, Tang L, Nguyen K. Development of a temperature-sensitive composite hydrogel for drug delivery applications. *Biotechnol Prog* 2006;22(1):118–125. [PubMed: 16454501]
2. Quick D, Anseth K. DNA delivery from photocrosslinked PEG hydrogels: encapsulation efficiency, release profiles, and DNA quality. *J Control Release* 2004;96:341–351. [PubMed: 15081223]
3. Mellott MB, Searcy K, Pishko MV. Release of protein from highly cross-linked hydrogels of poly(ethylene glycol) diacrylate fabricated by UV polymerization. *Biomaterials* 2001 May;22(9):929–941. [PubMed: 11311012]
4. Elisseeff J, McIntosh W, Anseth K, Riley S, Ragan P, Langer R. Photoencapsulation of chondrocytes in poly(ethylene oxide)-based semi-interpenetrating networks. *J Biomed Mater Res* 2000;51:164–171. [PubMed: 10825215]
5. Bryant S, Anseth K. The effects of scaffold thickness on tissue engineered cartilage in photocrosslinked poly(ethylene oxide) hydrogels. *Biomaterials* 2001;22:619–626. [PubMed: 11219727]
6. Masters K, Leibovich S, Belem P, West J, Poole-Warren L. Effects of nitric oxide releasing poly(vinyl alcohol) hydrogel dressing on dermal wound healing in diabetic mice. *Wound Repair Regen* 2002;10:286–294. [PubMed: 12406164]
7. Fisher J, Dean D, Mikos A. Photocrosslinking characteristics and mechanical properties of diethyl fumarate/poly(propylene fumarate) biomaterials. *Biomaterials* 2002;23:4333–4343. [PubMed: 12219823]
8. Yang F, Williams C, Wang D, Lee H, Manson P, Elisseeff J. The effect of incorporating RGD adhesive peptide in polyethylene glycol diacrylate hydrogel on osteogenesis of bone marrow stromal cells. *Biomaterials* 2005;26:5991–5998. [PubMed: 15878198]
9. Cruise G, Hegre O, Scharp D, Hubbell J. A sensitivity study of the key parameters in the interfacial photopolymerization of the poly(ethylene glycol) diacrylate upon porcine islets. *Biotechnol Bioeng* 1998;57:655–665. [PubMed: 10099245]
10. Cruise G, Hegre O, Lamberti F, Hager S, Hill R, Scharp D, et al. *In vitro* and *in vivo* performance of porcine islets encapsulated in interfacially photopolymerized poly(ethylene glycol) diacrylate membranes. *Cell Transplant* 2000;8:293–306. [PubMed: 10442742]
11. Burdick J, Anseth K. Photoencapsulation of osteoblasts in injectable RGD-modified PEG hydrogels for bone tissue engineering. *Biomaterials* 2002;23:4315–4323. [PubMed: 12219821]
12. Bryant S, Chowdhury T, Lee D, Bader D, Anseth K. Crosslinking density influences chondrocyte metabolism in dynamically loaded photocrosslinked poly(ethylene glycol) hydrogels. *Ann Biomed Eng* 2004;32:407–417. [PubMed: 15095815]
13. Gonzalez A, Gobin A, West J, McIntire L, Smith C. Integrin interactions with immobilized peptides in polyethylene glycol diacrylate hydrogels. *Tissue Eng* 2004;10:1775–1785. [PubMed: 15684686]
14. Kizilel S, Pérez-Luna V, Teymour F. Photopolymerization of poly(ethylene glycol) diacrylate on eosinfunctionalized surfaces. *Langmuir* 2004;20:8652–8658. [PubMed: 15379488]
15. Leach JB, Schmidt CE. Characterization of protein release from photocrosslinkable hyaluronic acid-polyethylene glycol hydrogel tissue engineering scaffolds. *Biomaterials* 2005 Jan;26(2):125–135. [PubMed: 15207459]
16. Masters K, Lipke E, Rice E, Liel M, Myler H, Zygorakis C, et al. Nitric oxide generating hydrogels inhibit neointima formation. *J Biomater Sci Polym Ed* 2005;16:659–672. [PubMed: 16001723]
17. Kopecek J, Yang J. Hydrogels as smart biomaterials. *Polym Int* 2007;56:1078–1098.
18. Ito S, Ronbunshu K. Phase Transition of Aqueous Solution of Poly(N-isopropylacrylamide) Derivatives—Effects of Side Chain Structure. *CSA Illumina* 1989;46(7):437–443.
19. Kavanagh C, Rochev Y, Gallagher W, Dawson K, Keenan A. Local drug delivery in restenosis injury: thermoresponsive co-polymers as potential drug delivery systems. *Pharmacol Ther* 2004;102(1):1–15. [PubMed: 15056495]

20. Luscher T, Steffel J, Eberli F, Joner M, Nakazawa G, Tanner F, et al. Drug-eluting stent and coronary thrombosis: biological mechanisms and clinical implications. *Circulation* 2007;115(8):1051–1058. [PubMed: 17325255]
21. Leon M. Late thrombosis a concern with drug-eluting stents. *J Interv Cardiol* 2007;20(1):26–29. [PubMed: 17300394]
22. Wenaweser P, Dorffler-Melly J, Imboden K, Windecker S, Togni M, Meier B, et al. Stent thrombosis is associated with an impaired response to antiplatelet therapy. *J Am Coll Cardiol* 2005;45(11):1748–1752. [PubMed: 15936599]
23. Braddock M, Campbell C, Zuder D. Current therapies for wound healing: electrical stimulation, biological therapeutics, and the potential for gene therapy. *Int J Dermatol* 1999;38(11):808–817. [PubMed: 10583612]
24. Indolfi C, Coppola C, Torella D, Arcucci O, Chiariello M. Gene therapy for restenosis after balloon angioplasty and stenting. *Cardiol Rev* 1999;7(6):324–331. [PubMed: 11208244]
25. Ishihara M, Nakanishi K, Ono K, Sato M, Kikuchi M, Saito Y, et al. Photocrosslinkable chitosan as a dressing for wound occlusion and accelerator in healing process. *Biomaterials* 2002;23(3):833–840. [PubMed: 11771703]
26. Shen Z, Terao K, Maki Y, Dobashi T, Ma G, Yamamoto T. Synthesis and phase behavior of aqueous poly(N-isopropylacrylamide-co-acrylamide), poly(N-isopropylacrylamide-co-N,N-dimethylacrylamide) and poly(N-isopropylacrylamide-co-2-hydroxyethylmethacrylate). *Colloid Polym Sci* 2006;284:1001–1007.
27. Bae YH, Okano T, Hsu R, Kim SW. Thermo-sensitive polymers as on-off switches for drug release. *Die Makromolekulare Chemie* 1987;8(10):481–485.
28. Bae YH, Okano T, Kim SW. “On-off” thermocontrol of solute transport. II. Solute release from thermosensitive hydrogels. *Pharm Res* 1991 May;8(5):624–628. [PubMed: 1866377]
29. Hoffman AS. Applications of thermally reversible polymers and hydrogels in therapeutics and diagnostics. *J Control Release* 1987;6(1):297–305.
30. Hoffman, AS.; Stayton, PS.; Bulmus, V.; Chen, G.; Chen, J.; Cheung, C., et al. Really smart bioconjugates of smart polymers and receptor proteins. *J Biomed Mater Res; Founder’s Award, Society for Biomaterials. Sixth World Biomaterials Congress 2000; Kamuela, HI. May 15-20, 2000; 2000 Dec 15. p. 577-586.*
31. Huang G, Gao J, Hu Z, St John JV, Ponder BC, Moro D. Controlled drug release from hydrogel nanoparticle networks. *J Control Release* 2004 Feb 10;94(23):303–311. [PubMed: 14744482]
32. Xia X, Hu Z, Marquez M. Physically bonded nanoparticle networks: a novel drug delivery system. *J Control Release* 2005 Mar 2;103(1):21–30. [PubMed: 15710497]
33. Waltera E, Moelling K, Pavlovic J, Merkle HP. Microencapsulation of DNA using poly(DL-lactide-co-glycolide): stability issues and release characteristics. *J Control Release* 1999;61:361–374. [PubMed: 10477808]
34. DeLong S, Moon J, West J. Covalently immobilized gradients of bFGF on hydrogel scaffolds for directed cell migration. *Biomaterials* 2005;26(16):3227–3234. [PubMed: 15603817]
35. Nuttelman C, Tripodi M, Anseth K. In vitro osteogenic differentiation of human mesenchymal stem cells photoencapsulated in PEG hydrogels. *J Biomed Mater Res A* 2004;68(4):773–782. [PubMed: 14986332]
36. Caykara T, Kiper S, Demirel G. Thermosensitive poly(N-isopropylacrylamide-co-acrylamide) hydrogels: Synthesis, swelling and interaction with ionic surfactants. *Eur Poly J* 2006;42:348–355.
37. Sabnis A, Chapman C, Rahimi M, Nguyen KT. Cytocompatibility Studies of an in situ Photopolymerized Thermoresponsive Hydrogel Nanoparticle System using Human Aortic Smooth Muscle Cells. *J Biomed Mater Res A*. In press
38. Ghosh K, Shu X, Mou R, Lombardi J, Prestwich G, Rafailovich M, et al. Rheological characterization of in situ cross-linkable hyaluronan hydrogels. *Biomacromolecules* 2005;6(5):2857–2865. [PubMed: 16153128]
39. Kim SW, Bae YH, Okano T. Hydrogels: swelling, drug loading, and release. *Pharm Res* 1992 Mar; 9(3):283–290. [PubMed: 1614957]

40. Diramio J, Kisaalita W, Majetich G, Shimkus J. Poly(ethylene glycol) methacrylate/dimethacrylate hydrogels for controlled release of hydrophobic drugs. *Biotechnol Prog* 2005;21(4):1281–1288. [PubMed: 16080712]

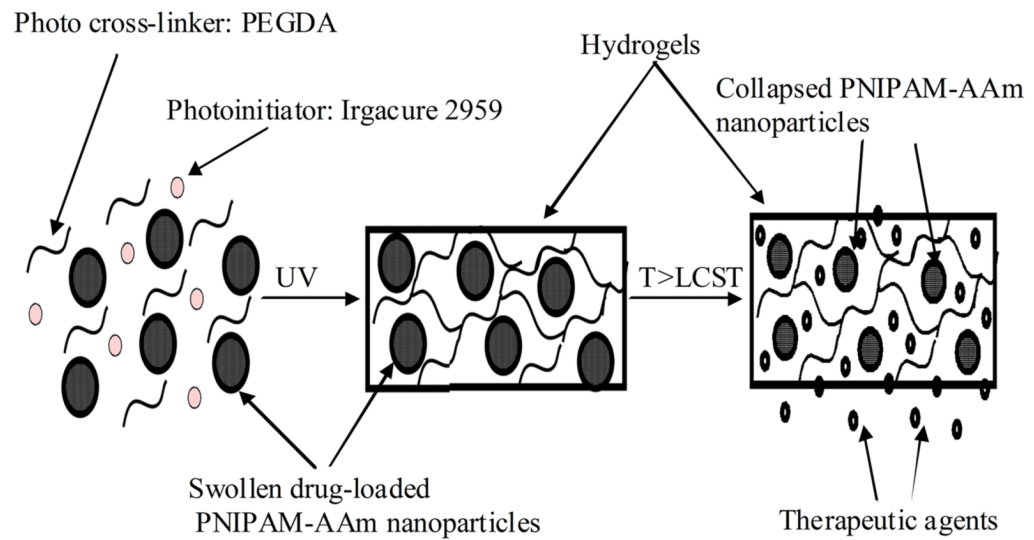


Figure 1. Principle of the photopolymerizable thermoresponsive composite nanoparticle hydrogels

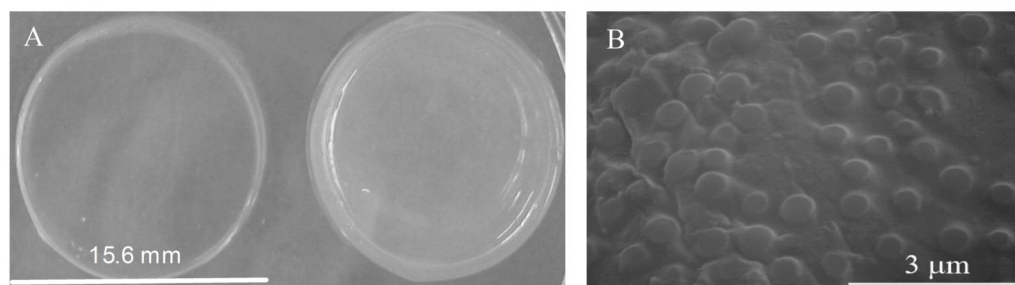
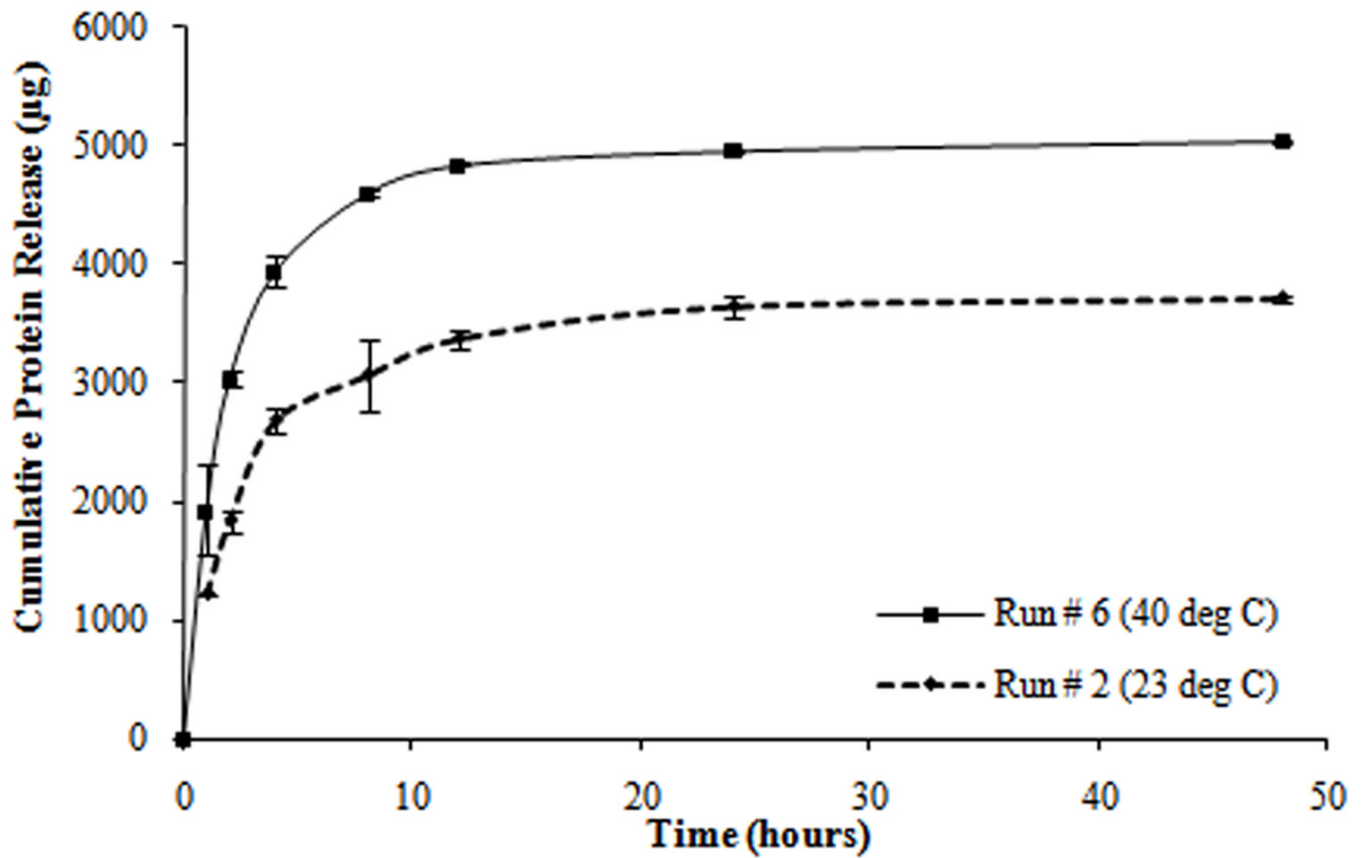
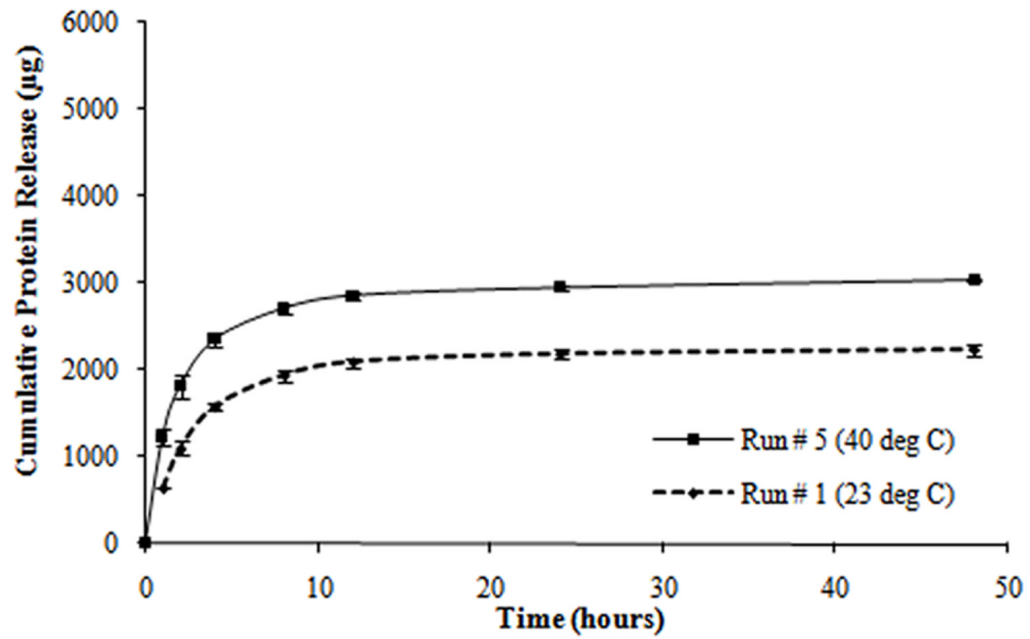


Figure 2. (a) Comparison of identical composite nanoparticle hydrogels incubated at 23°C (left) and 40°C (right); (b) SEM image of composite nanoparticle hydrogels with 20% (w/v) PNIPAM-AAm nanoparticles



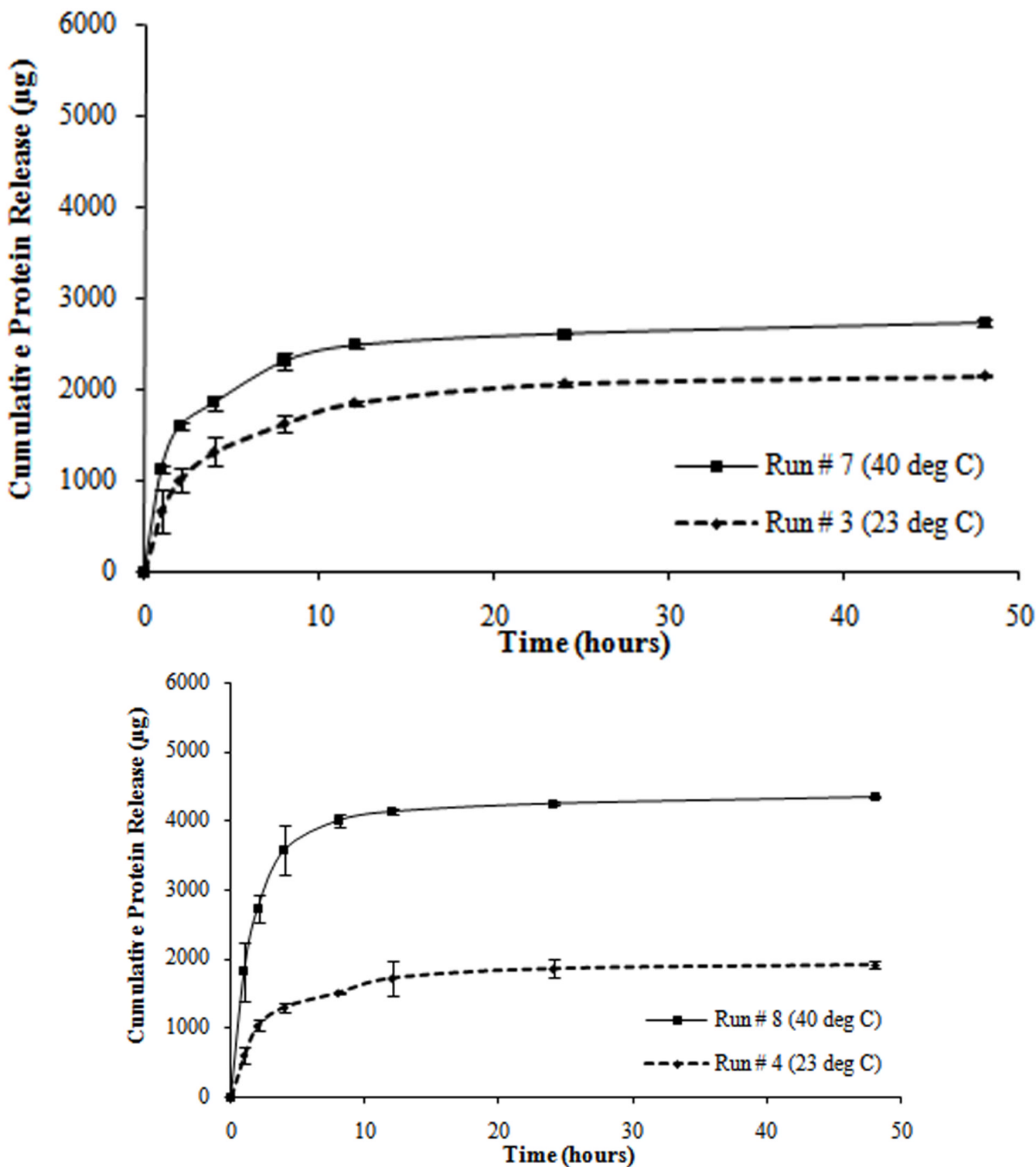
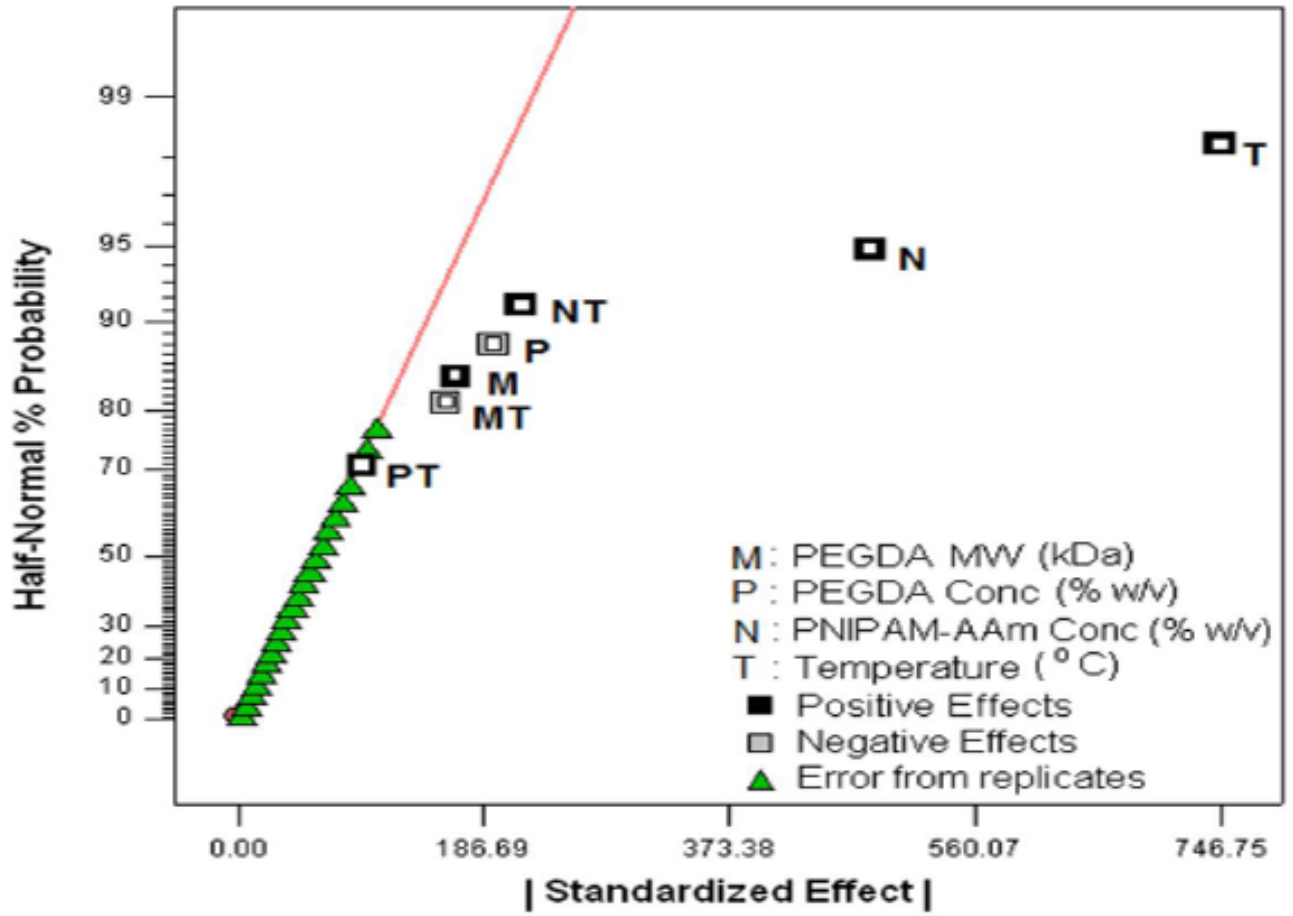
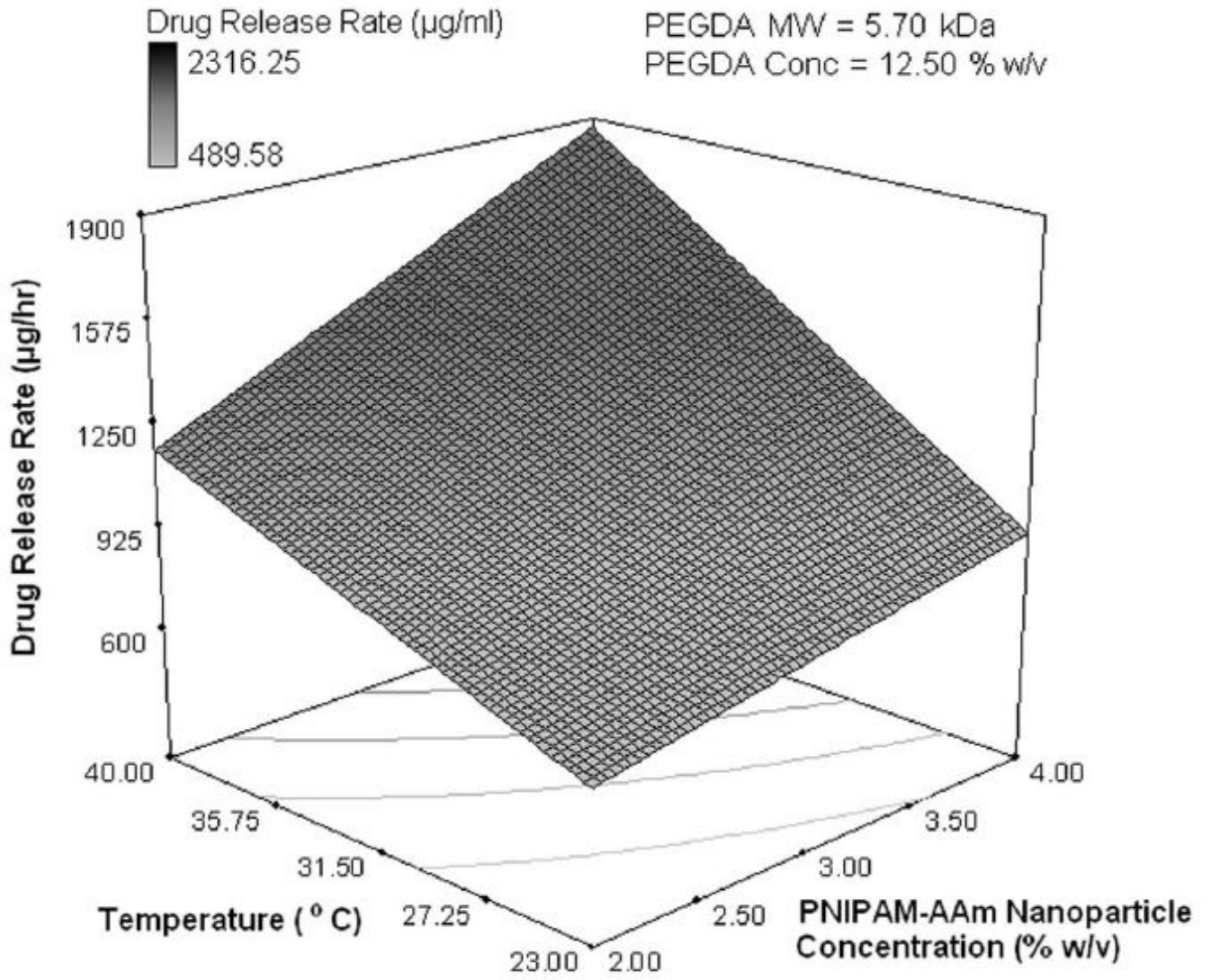
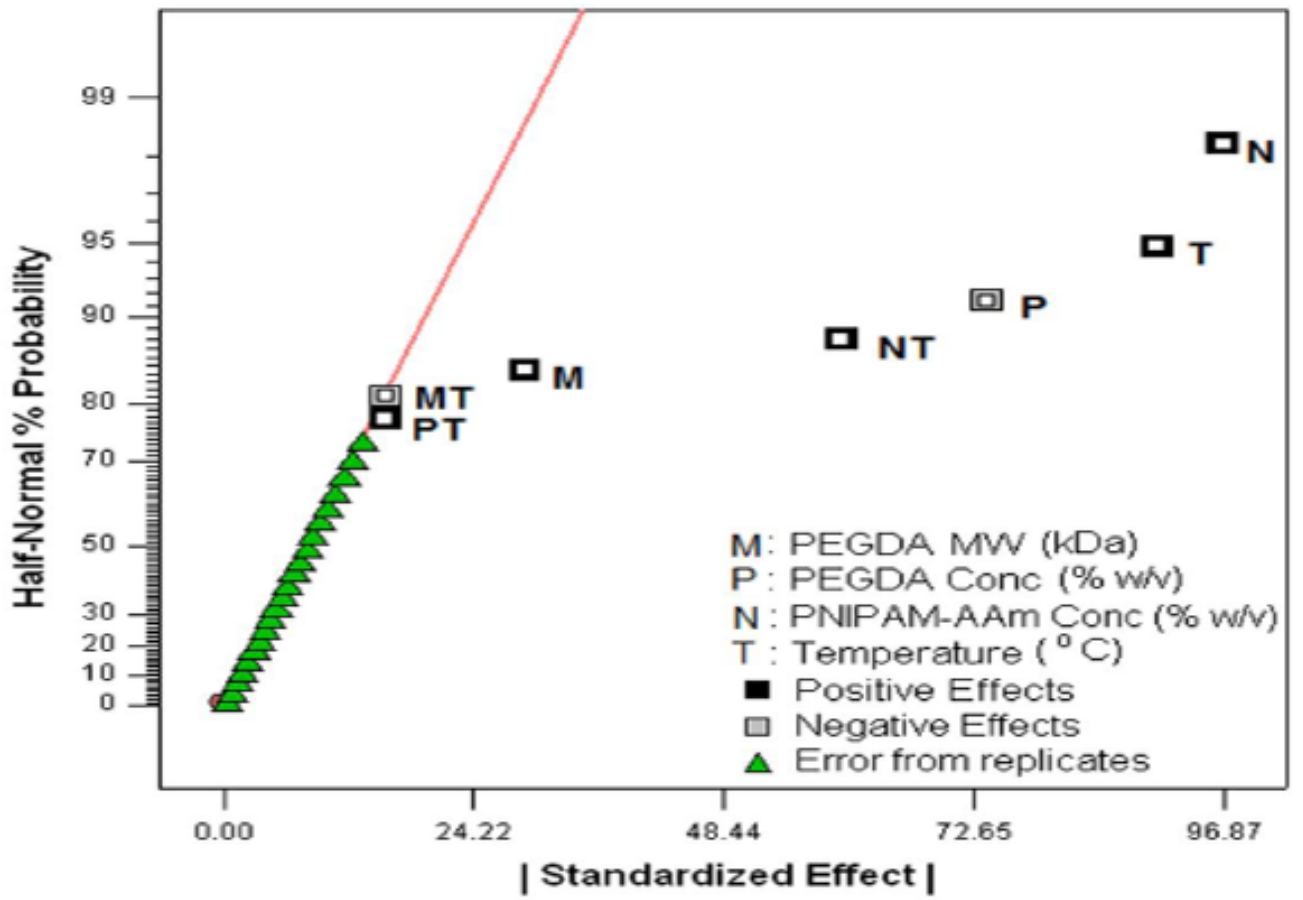


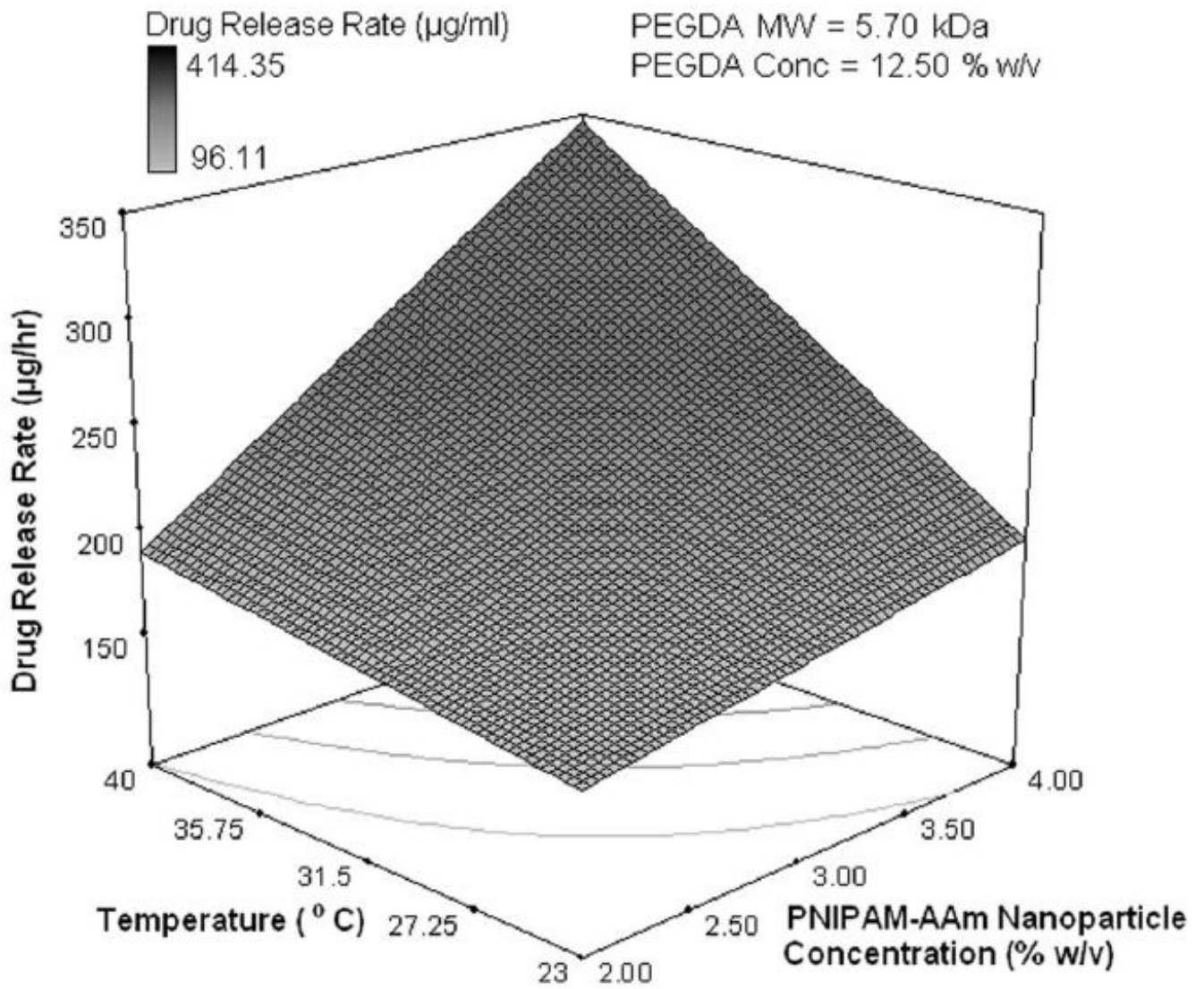
Figure 3. Protein release profiles for different composite hydrogels formulated as shown in Table 2. (a) Hydrogels with the molecular weight of PEGDA (M) at 3.4 kDa, the concentration of PEGDA (P) at 10% w/v, and the concentration of PNIPAM-AAm nanoparticles (N) at 2% w/v. (b)

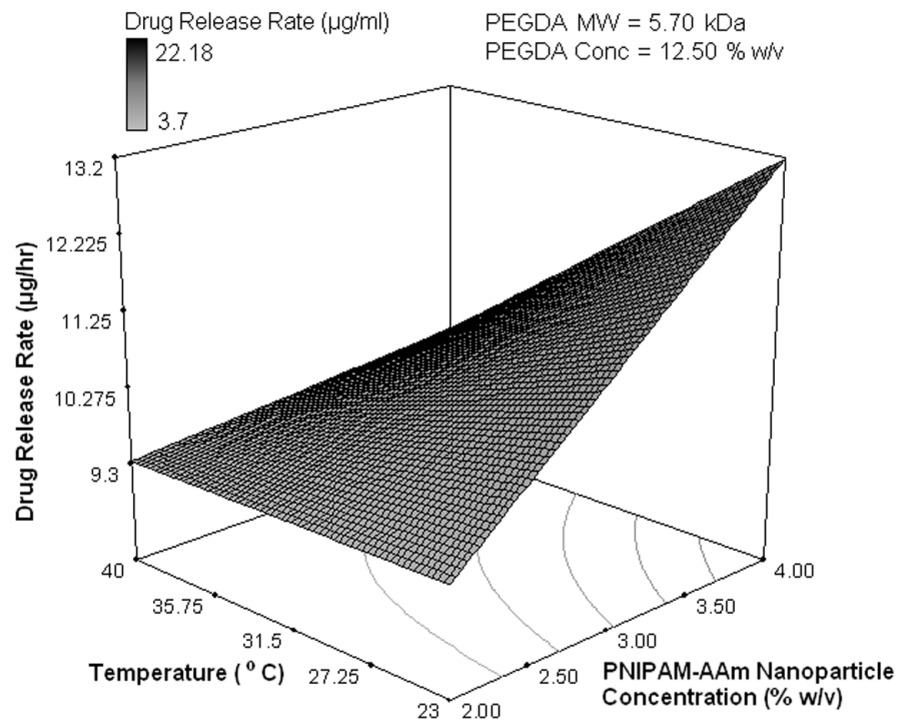
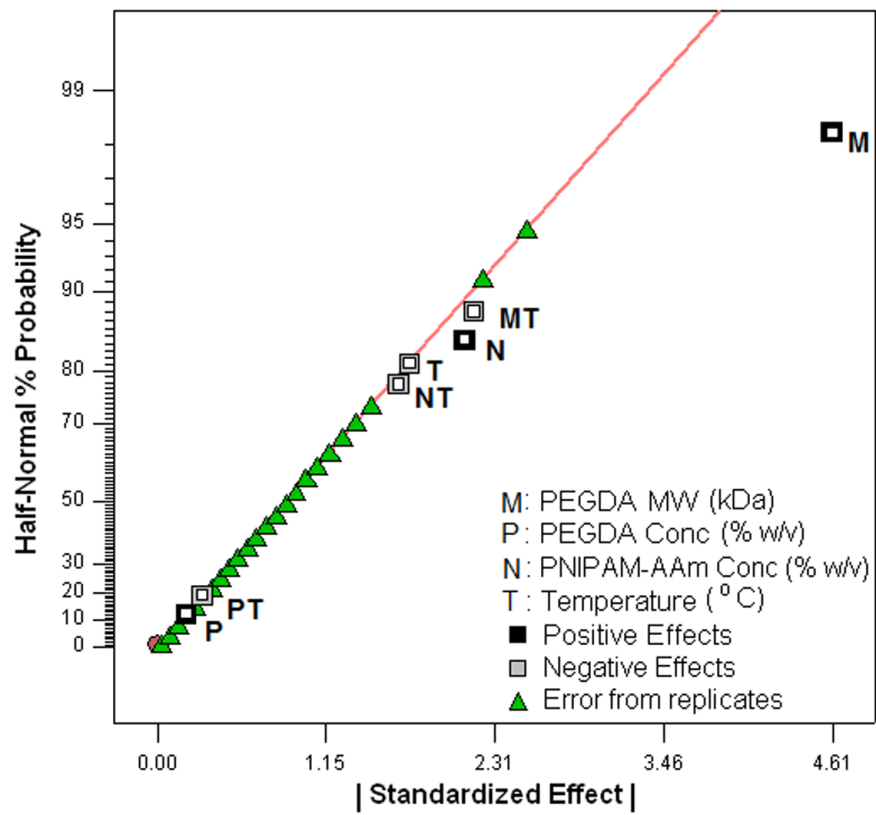
Hydrogels with M at 8 kDa, P at 10% w/v, and N at 4% w/v. (c) Hydrogels with M at 8 kDa, P at 15% w/v, and N at 2% w/v. (d) Hydrogels with M at 3.4 kDa, P at 15% w/v, and N at 4% w/v.

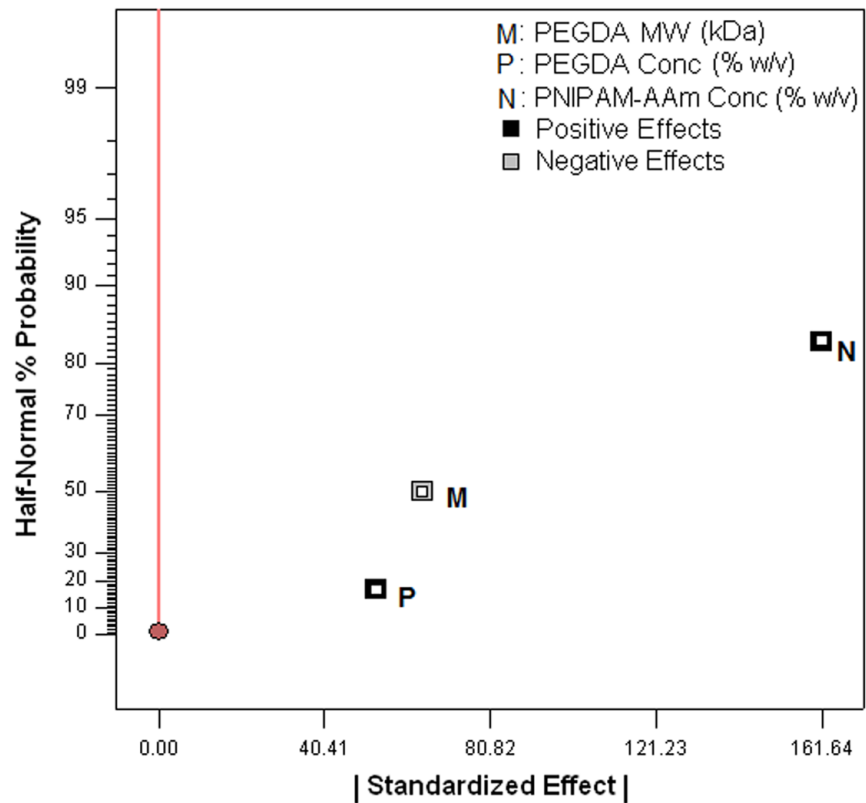
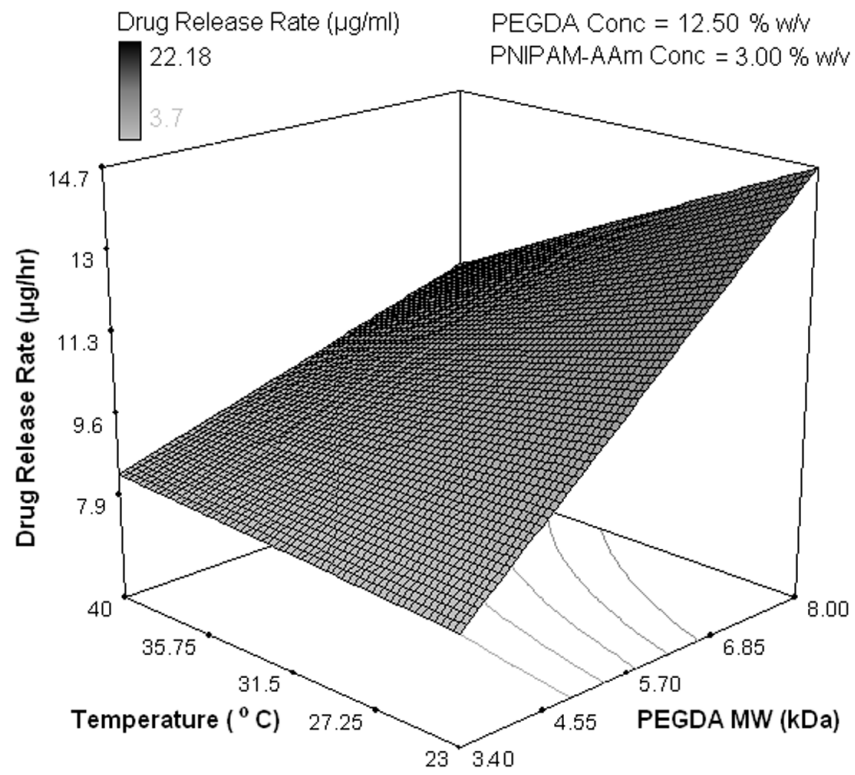












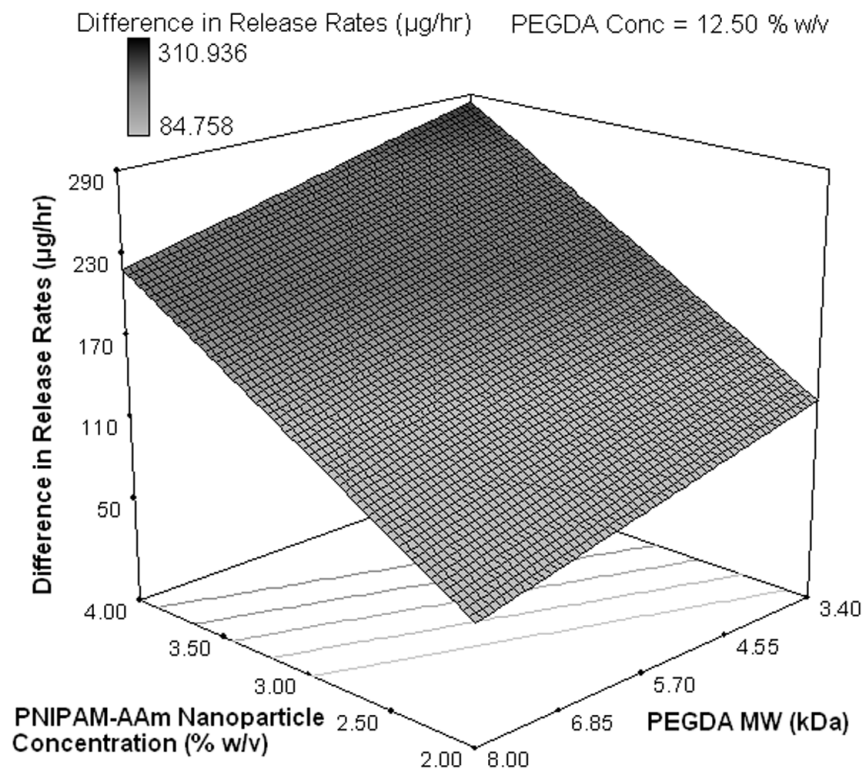


Figure 4.

Half-normal plot showing the effect of factors on the (a) protein release rate in phase I (burst release), (c) protein release rate in phase II (sustained burst release), (e) protein release rate in phase III (plateau release), and (h) thermoresponsiveness of the hydrogels (up to 8 hrs); 3D surface plot showing the effect of factors on the (b) protein release rate in phase I (burst release), (d) protein release rate in phase II (sustained burst release), (f, g) protein release rate in phase III (plateau release), and (i) thermoresponsiveness of the hydrogels (up to 8 hrs)

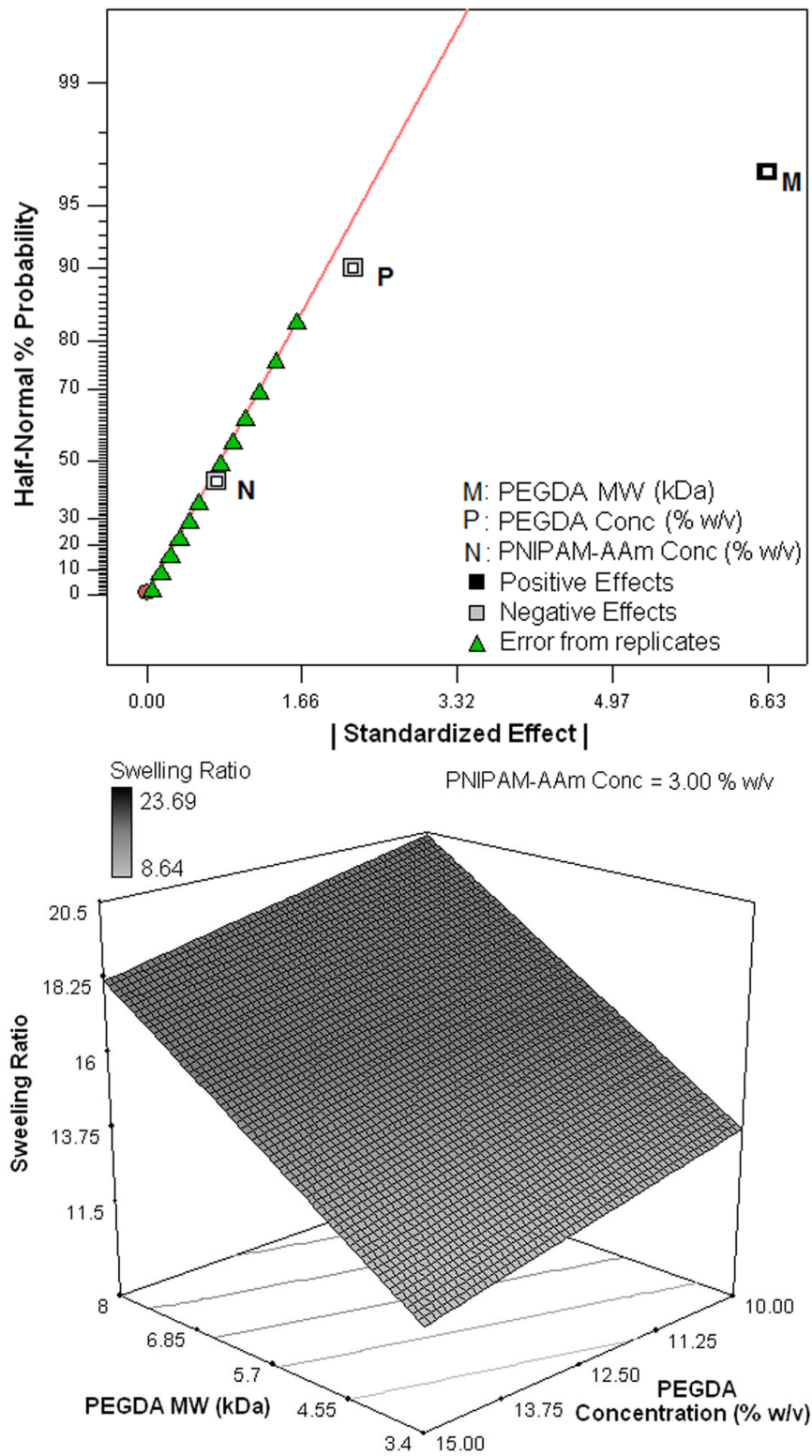


Figure 5. (a) Half-normal plot and (b) 3D surface plot showing the effect of the processing factors on the hydrogel swelling ratio

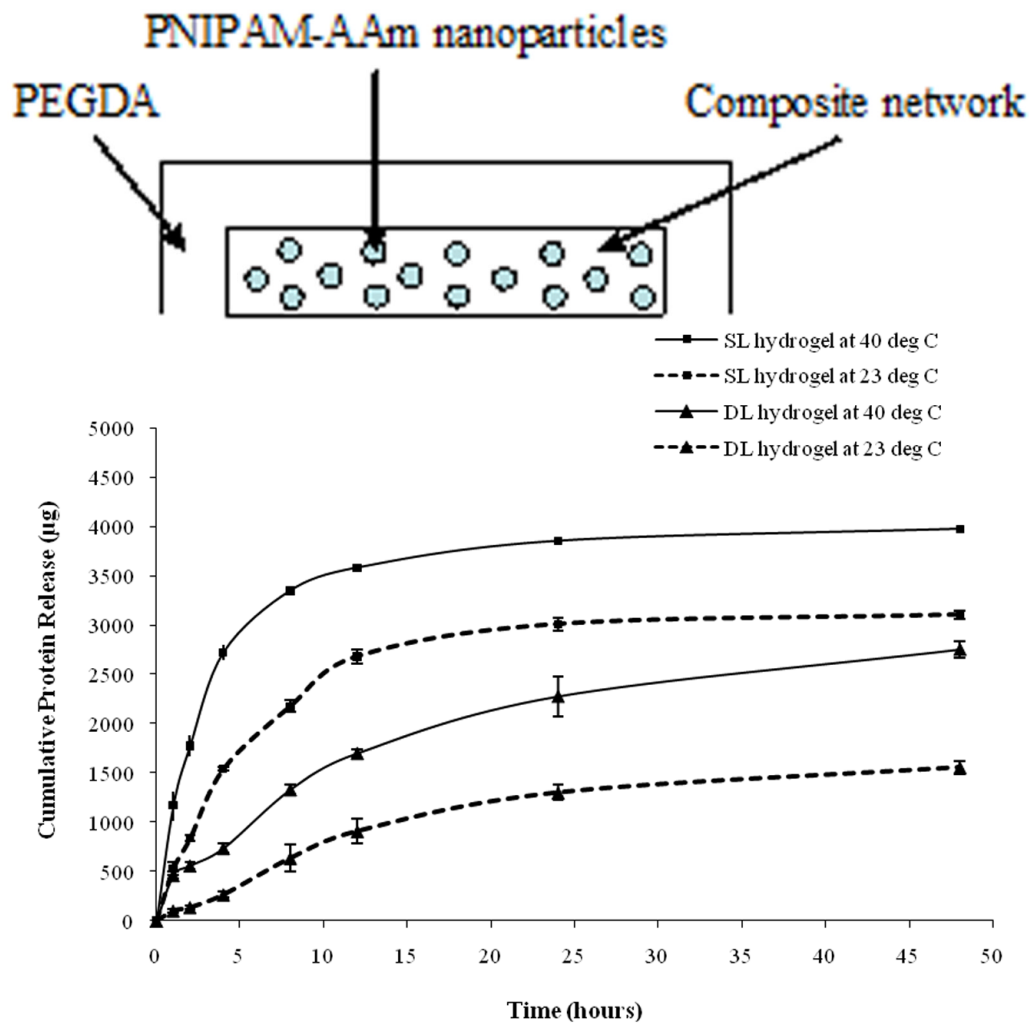


Figure 6. (a) Structure of the double layer composite nanoparticle hydrogel, (b) protein release profiles of single layer (SL) and double layer (DL) hydrogels at 23°C and 40°C

Table 1

Low and high levels for the half factorial design, where M is the molecular weight of PEGDA, P is the concentration of PEGDA, N is the concentration of PNIPAM-AAm nanoparticles, and T is the temperature

Level	M (kDa)	P (% w/v)	N (% w/v)	T (°C)
Low (0)	3.4	10	2	23
High (1)	8.0	15	4	40

Table 2

Actual values of the half 4-factor design; and the protein release rate over a time course of the single layer hydrogels

Run #	M (kDa)	P (% w/v)	N (% w/v)	T (°C)	Protein Release Rate (µg/hr)		
					0-1 hour	1-8 hours	8-48 hours
1	3.4	10	2	23	644	185	7.3
2	8.0	10	4	23	1216	264	16.3
3	8.0	15	2	23	663	13	13.0
4	3.4	15	4	23	603	129	10.0
5	3.4	10	2	40	1222	212	8.2
6	8.0	10	4	40	1927	383	11.1
7	8.0	15	2	40	1128	167	10.5
8	3.4	15	4	40	1818	311	8.5

Table 3

Actual values of the half 3-factor design; and the swelling ratio of the single layer hydrogels

Run #	M (kDa)	P (% w/v)	N (% w/v)	Swelling Ratio
1	3.4	10	2	12.79
2	8.0	10	4	19.05
3	8.0	15	2	17.31
4	3.4	15	4	9.95